Morel et al., *Cogent Chemistry* (2015), 1: 1070943
http://dx.doi.org/10.1080/23312009.2015.1070943

cogent chemistry

PHYSICAL CHEMISTRY | RESEARCH ARTICLE

Thermodynamics of selenium sorption on alumina and montmorillonite

Jean-Pierre Morel[1], Nicolas Marmier[2], Charlotte Hurel[2] and Nicole Morel-Desrosiers[1]*

Received: 14 March 2015
Accepted: 01 July 2015
Published: 17 August 2015

*Corresponding author: Nicole Morel-Desrosiers, Université Clermont Auvergne - Université Blaise Pascal, Laboratoire Microorganismes: Génome et Environnement, UMR CNRS 6023, BP 10448, 63000 Clermont-Ferrand, France
E-mail: Nicole.MOREL@univ-bpclermont.fr

Reviewing editor:
Mark Russell St. John Foreman, Chalmers University of Technology, Sweden

Additional information is available at the end of the article

Abstract: The effect of pH and temperature on the thermodynamics of selenium sorption on alumina and montmorillonite was investigated. The equilibrium constants were obtained from batch experiments carried out at 25 and 40°C, under acidic and near to neutral conditions. Microcalorimetry was used to measure directly the enthalpy change upon sorption. These data were analysed by taking into account the different reactions that occur during the sorption process (the acid–base equilibria in the bulk solution on the one hand and the complexation equilibria between surface sites of the solid and solution species on the other hand). This was done using a simple surface model which assumes that the thermodynamic properties of the aluminol surface sites of both alumina and montmorillonite are identical. Two of the considered reactions were found to predominate, one under acidic conditions and one at near neutral pH. The microcalorimetric data allowed to check that the temperature effect on selenium sorption on alumina and montmorillonite can be correctly predicted simply using the above assumption concerning the sorption sites and by applying van't Hoff relation both to the homogeneous and heterogeneous reactions.

Subjects: Analytical Chemistry; Environmental Chemistry; Physical Chemistry

Keywords: selenium; sorption; temperature effect; pH effect; surface complexation model; alumina; montmorillonite; enthalpy of sorption; microcalorimetry; selenium speciation

ABOUT THE AUTHORS

Nicole Morel-Desrosiers and Jean-Pierre Morel are thermodynamicists involved in the microcalorimetric determination of the energetic parameters characterizing processes such as the formation of supramolecular complexes in solution, the exchanges at the solid–liquid and liquid–liquid interfaces, and the metabolic activity of micro-organisms. Charlotte Hurel and Nicolas Marmier are involved in the understanding of surface interactions between synthetic or natural solids and inorganic/organic pollutants. Their research activity consists in macroscopic investigations and thermodynamic modelling on the basis of surface complexation theory.

PUBLIC INTEREST STATEMENT

Selenium is an essential micronutrient for humans and animals but it can be highly toxic depending on its chemical form (oxidation state) and concentration. It naturally occurs at low level but anthropogenic activities such as mining and combustion of fossil fuels can highly increase its concentration in the different compartments of the environment (soil, water and air). The chemical forms which are water-soluble can also bind, more or less strongly, to the organic matter, metal oxides and clay minerals present in the soils. Aquatic organisms and plants can bioaccumulate the soluble and mobile forms of selenium and thus contaminate the food web. The partitioning of selenium between mineral surfaces and water depends largely on the physicochemical conditions. The present study aims at acquiring the thermodynamic data necessary to understand how this partitioning is modified when the temperature increases and the acidity of the medium changes.

1. Introduction

Selenium, a sulphur analogue, is a natural trace element found in bedrock, or introduced into the environment by anthropogenic activities such as mining and combustion of fossil fuels (Wen & Carignan, 2007). It is an essential micronutrient at low concentrations but it can cause adverse effects if its consumption is not moderate (Tinggi, 2003). Selenium toxicity depends on its speciation and on its dose (Ma et al., 2012). The speciation strongly depends on the redox and pH of the environment (de Llano, Bidoglio, Avogadro, Gibson, & Rivas Romero, 1996; Kumar & Riyazuddin, 2011; Ryu, Gao, & Tanji, 2011; Séby, Potin Gautier, Lespés, & Astruc, 1997; Torres et al., 2011). Selenium can be found in four oxidation states: selenide (Se^{2-}), elementary selenium (Se^{0}), selenite (SeO_3^{2-}) and selenate (SeO_4^{2-}) (Bingham, Connelly, Cassingham, & Hyatt, 2010). Selenite and selenate are water-soluble but can also bind, more or less strongly, to the organic matter, metal oxides and clay minerals present in the soils. The selenite form was found to be more toxic and more mobile than the selenate form (Fujimoto, Morinaga, Abe, Kitamura, & Sakuma, 2009; Johnston, 1987; Morlon et al., 2005). The partition of selenium between mineral surfaces and water is an important question since aquatic organisms and plants can bioaccumulate the soluble and mobile forms. This partitioning largely depends on the physicochemical conditions of the environment.

Adsorption experiments are generally conducted in order to evaluate the partition of ions between mineral surfaces and water, under various physicochemical conditions such as pH, ionic strength, initial concentration of ions, etc. The experimental adsorption data are commonly described according to the surface complexation model (SCM) (Cornelis et al., 2008; Goldberg, Lesch, & Suarez, 2007; Jordan, Marmier, Lomenech, Giffaut, & Ehrhardt, 2009). This approach (general composite) implies that generic surface sites (strong sites and/or weak sites) and surface species are used. The surface properties (surface sites concentration, acidity constants) of the generic sites are obtained from numerical fit of potentiometric titrations carried out on the adsorbent phase (clay, iron oxyhydroxides), and the surface species are deduced from surface spectroscopy and/or from adsorption data experimentally obtained on the adsorbent phase (Davis, Meece, Kohler, & Curtis, 2004; Um, Serne, Brown, & Rod, 2008). The major disadvantage of this procedure is that no independent verification of the surface characteristics is possible since surface properties and thermodynamic constants are correlated to each other and are adsorbent dependent. Another approach (component additivity) of the SCM consists in the description of the complex surface as the sum of individual single oxides (Alessi & Fein, 2009; Schaller, Koretsky, Lund, & Landry, 2009). This surface description presents the advantage that acid–base properties and adsorption constants can be independently deduced from experiments carried out on each single oxide. Even if this approach is a simplified consideration of a complex surface because it does not account for the crystallography of the complex solid itself, it allows the use of common thermodynamic data related to single oxides, and the adjustment procedure of the calculations can be largely reduced (Landry, Koretsky, Lund, Schaller, & Das, 2009).

Irrespectively of the modelling assumptions, until now, most of the studies concerning ion adsorption on mineral surfaces were investigated at ambient temperature, and the proposed thermodynamic data concerning surface sites and surface species (pK_a and adsorption pK) were valid only at 25°C. To propose reliable models able to model experimental data in a large temperature range, it is of great importance to measure thermodynamic data such as enthalpies of protonation–deprotonation and enthalpies of adsorption.

In the present work, adsorption of SeO_3^{2-} was investigated at 25 and 40°C on alumina and montmorillonite. Selenium was chosen because (i) of its high affinity for the alumina surface, and (ii) of selective adsorption of selenium on the aluminol sites of the montmorillonite. Enthalpy of protonation–deprotonation and enthalpy of Se(IV) adsorption were microcalorimetrically determined at 25°C for the two systems: alumina–selenium and montmorillonite–selenium. Adsorption experiments of Se(IV) were then investigated on alumina and montmorillonite, at 25 and 40°C.

The van't Hoff equation was used to determine the aqueous and surface constants (K) at 40°C from the measured enthalpies.

Finally, the component additivity of the SCM was used in order to predict adsorption of Se(IV) on alumina–selenium and montmorillonite–selenium systems without adjustment of the thermodynamic constant determined elsewhere. The thermodynamic data were determined following the experiments carried out on the alumina single oxide and, as regards the components additivity approach, mass action law (MAL) data were extended to montmorillonite without any adjustment.

2. Materials and methods

2.1. Reagents

A synthetic γ 90 alumina (Merck, aluminium oxide standardized 90) and a purified and sodic MX-80 montmorillonite (Wyoming), designed as MNa throughout this paper, were used in the present study. The characteristics and properties of both solids (Morel, Marmier, Hurel, & Morel-Desrosiers, 2006, 2012) are given in Table 1.

The selenium stock solution (10^{-2} mol L^{-1}) was obtained by dissolution in pure water of Na_2SeO_3 provided by Alfa Aesar.

The microcalorimetric and batch experiments were carried out in a 0.100 mol L^{-1} $NaNO_3$ aqueous solution. Nitric acid (1 mol L^{-1}) and sodium hydroxide (1 mol L^{-1}) solutions were used to adjust the pH value of each alumina and montmorillonite suspensions.

2.2. Batch experiments

The sorption of Se(IV) on alumina and montmorillonite was studied as a function of pH, under atmospheric conditions, at 25 and 40°C. The experiments were performed in 50-mL batch vessels placed in an incubator equipped with an elliptic shaker (CERTOMAT *IS* B. Braun Biotech International), in order to keep constant the temperature during the experiments, and also a constant agitation. In order to work with the same Se/aluminol sites ratio for both alumina and montmorillonite surfaces, the Se(IV) initial concentration was 2.5×10^{-3} mol L^{-1} and the solid-to-liquid ratio was 4 g L^{-1} for the experiments on alumina, and the Se(IV) initial concentration was 2.5×10^{-4} mol L^{-1} and the solid-to-liquid ratio was 40 g L^{-1} for the experiments on montmorillonite. The pH of each suspension was adjusted between 2 and 10 by adding microvolumes of HNO_3 or NaOH solutions. Seven days of shaking (4,000 rpm) at constant temperature were necessary to get an equilibrated system. The pH of each suspension was then measured with a pH-meter (WTW pH 340) equipped with a combined pH electrode, previously calibrated at the temperature of each experiment following the procedure described previously (Morel et al., 2006; Morel, Marmier, Hurel, & Morel-Desrosiers, 2009). Then, the liquid and the solid phases were separated in a thermostatic centrifuge (SIGMA 3-30K) and aliquots were filtered through a 0.45-µm porosity membrane (minisart RC-25 Sartorius). The filtrated solutions were then acidified to pH 2 with concentrated HNO_3 (65%), before analysis of selenium by ICP-AES (Perkin-Elmer Optima 7300DV) using external calibration.

2.3. Microcalorimetric titrations

Our purpose was to measure directly the enthalpy change associated with the sorption of SeO_3^{2-} on the aluminol edge sites of MNa on the one hand, and on the aluminol sites of γ-Al_2O_3 on the other hand.

Table 1. Characteristics and properties of alumina and Na-montmorillonite at 25°C

	Alumina	Na-montmorillonite
Provider	MERCK Alumina 90	Wyoming
Surface sites concentration	3.85×10^{-4} mol g^{-1}	3.75×10^{-6} mol g^{-1}
Surface sites density	1.7 sites nm^{-2}	
Specific area	135.5 m^2 g^{-1}	30.0 m^2 g^{-1}
pH_{zpc}	8.6	

In order to do so, we have titrated both suspensions under similar conditions, and in particular at identical aluminol sites concentrations.

The heats have been measured at 25°C with a twin thermopile heat-conduction isothermal TAM 2277 microcalorimeter (Thermometric – TA Instruments) following the titration technique previously described (Morel et al., 2006, 2009, 2012). The microcalorimetric titration has been carried out as follows: 3 mL of the suspension has been put in a 4-mL stainless steel ampoule and the equilibrated system has been titrated by 20 successive injections of 10 µL of the SeO_3^{2-} aqueous solution. The injections have been made using a precision Lund pump (Thermometric – TA Instruments) equipped with a 250-µL Hamilton syringe fitted with a gold cannula.

We know that the sorption of the selenite ions on the aluminol sites occurs in acidic medium. Different titration conditions have been examined in order to choose the one that is the most adapted to our purpose and to the constraints of the experimental device. The aluminol sites density being equal to 3.75×10^{-6} mol g^{-1} for MNa (Hurel et al., 2002) and to 3.85×10^{-4} mol g^{-1} for γ-Al_2O_3 (Marmier, Dumonceau, Chupeau, & Fromage, 1994), the two solids have been suspended at concentrations of 40 g L^{-1} and 0.40 g L^{-1}, respectively. Under these conditions, the aluminol sites concentration is almost the same in both cases, that is 1.5×10^{-4} mol L^{-1}. Some titrations have also been carried out at a concentration of 4 g L^{-1} in order to study the effect of the aluminol sites concentration. No particular problem has been encountered due to the relatively high mass concentration. As in our previous works (Morel et al., 2006, 2009, 2012), the suspensions have been prepared in 0.100 mol L^{-1} $NaNO_3$ aqueous solution, stirred for 5–6 days, and the aliquots have been taken under stirring conditions. The selenite species being negatively charged, the cation exchange sites of MNa are not involved in the titration process.

The titrant, which has been prepared in 0.100 mol L^{-1} $NaNO_3$ aqueous solution, contains equivalent concentrations of SeO_3^{2-} and H^+, that is 4.0×10^{-3} mol L^{-1} Na_2SeO_3 and 8.0×10^{-3} mol L^{-1} HNO_3. Upon both titrations, the pH of the suspension varies from 8.4 to 3.8, which enables the observation of the sorption of selenium in an appropriate way, as will be shown below through the speciation curves.

2.4. Modelling

The SCM used here assumes that a finite number of reactive sites are present on the solid surface (*S*) of alumina and montmorillonite. These aluminol sites (*SOH*), which are assumed to be present on both alumina and montmorillonite surfaces, are involved in protonation–deprotonation reactions, and may fix or release SeO_3^{2-} ions. The equations of the surface reactions concerning H^+, SeO_3^{2-} and *SOH* can be represented as follows:

- for the acid–base selenite reactions in aqueous solution (Séby, Potin-Gautier, Giffaut, Borge, & Donard, 2001):

$$SeO_3^{2-} + H^+ = HSeO_3^- \qquad K_1, \Delta H_1 \tag{1}$$

$$HSeO_3^- + H^+ = H_2SeO_3 \qquad K_2, \Delta H_2 \tag{2}$$

- for the acid–base surface reactions (Morel et al., 2012):

$$SO^- + H^+ = SOH \qquad K_3, \Delta H_3 \tag{3}$$

$$SOH + H^+ = SOH_2^+ \qquad K_4, \Delta H_4 \tag{4}$$

- for the surface complexation reactions, we considered the formation of selenite outer-sphere complex at the surface of alumina as suggested by (Peak, 2006):

$$SOH_2^+ + SeO_3^{2-} = SSeO_3^- + H_2O \qquad K_5, \Delta H_5 \tag{5}$$

$$SOH_2^+ + SeO_3^{2-} + H^+ = SSeO_3H + H_2O \qquad K_6, \Delta H_6 \tag{6}$$

The equilibrium constants used for the calculations are given in Table 2.

It should be noted that we have used the same K values for the sorption of selenium on the aluminol sites of both solids (Morel et al., 2012). In the present case, the electrostatic term is modelled using the diffuse layer model (DLM) (Lyklema, de Keizer, Bijsterbosch, Fleer, & Cohen Stuart, 1995). The FITEQL 4.0 calculation code (Herbelin & Westall, 1999) has been used to fit the experimental results of the batch experiments.

3. Results and discussion

3.1. Speciation curves

Figures 1 and 2 show the variation upon titration of the equilibrium concentrations of the species present in the solution and on the solid surface of montmorillonite and alumina, respectively. Apart for Na^+, NO_3^- and H^+, the following species are present: SeO_3^{2-}, $HSeO_3^-$ and H_2SeO_3 in the solution and SO^-, SOH, SOH_2^+, $SSeO_3^-$ and $SSeO_3H$ on the solid.

Figure 1, relating to MNa, leads to the following conclusions for the first half of the titration: in the solution, the concentration of the SeO_3^{2-} ions goes through a small maximum and then tends to zero, and the concentration of the protonated species $HSeO_3^-$ increases while the pH remains almost constant; on the solid, the SOH sites are progressively transformed into SOH_2^+ sites, and the SeO_3^{2-} ions of the solution do sorb as $SSeO_3^-$, whose concentration goes through a small maximum before tending to zero while the concentration of the protonated form $SSeO_3H$ increases regularly. So until pH 5 (that is, before the 10th injection), several species do coexist in the system and it is impossible to extract from the measured total heat the part due to the sorption of selenium. From the 10th injection, that is in acidic medium (pH decreases from 5 to 3.8), the situation is much simpler: in the solution, whereas the concentration of SeO_3^{2-} is equal to zero, the protonated form $HSeO_3^-$ continues to increase and the diprotonated form H_2SeO_3 does appear but its concentration increases very slowly; on the solid, the SOH sites are no more present and the SOH_2^+ sites decrease slowly, while the SeO_3^{2-} ions of the solution now do sorb only as $SSeO_3H$. So, in this pH range, only three simultaneous reactions need to be taken into account: reactions (1) and (2) for the first and second protonation of SeO_3^{2-} in the solution, and reaction (6) for the sorption of SeO_3^{2-} on the solid surface. This will allow us to extract ΔH_6 from the total heat measured during the second half of the titration.

Figure 2, relating to alumina, leads to the same observations. It can be noted, however, that the $SSeO_3H$ and $SSeO_3^-$ concentrations are larger: at the 20th injection, the $SSeO_3H$ concentration is almost thrice larger for Al_2O_3 than for MNa; between the 10th and 20th injections, the $SSeO_3^-$ concentration remains equal to zero for MNa whereas it starts at a non-negligible value for Al_2O_3 and then tends

Table 2. pKs for the alumina and Na-montmorillonite surfaces at 25 and 40°C, and I = 0.1 mol L^{-1}*

Reaction	ΔH (kJ mol^{-1})	pK 25°C	pK 40°C (calculated)
$SeO_3^{2-} + H^+ = HSeO_3^-$	−5.0	8.3	8.4
$HSeO_3^- + H^+ = H_2SeO_3$	6.2	2.4	2.3
$SO^- + H^+ = SOH$	−14	−9.2	−9.1
$SOH + H^+ = SOH_2^+$	−17	−7.9	−7.8
$SOH_2^+ + SeO_3^{2-} = SSeO_3^- + H_2O$	35	4.4	4.1
$SOH_2^+ + SeO_3^{2-} + H^+ = SSeO_3H + H_2O$	40	11.2	10.9

*The aluminol sites, designed by SOH, were considered identical for alumina and Na-montmorillonite (see text).

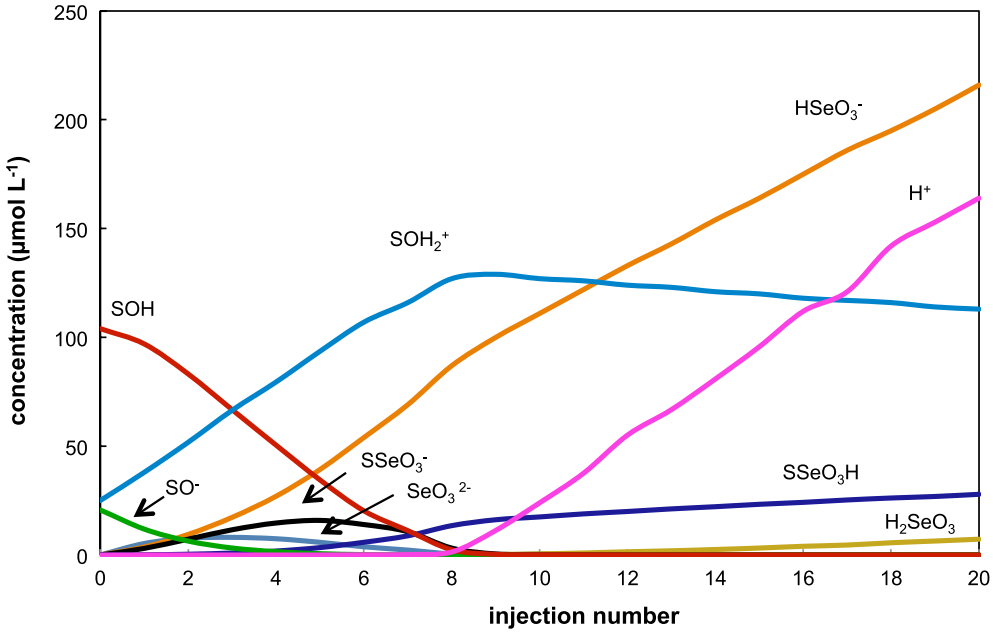

Figure 1. Aqueous and surface speciation curves for Na-montmorillonite and selenite system.

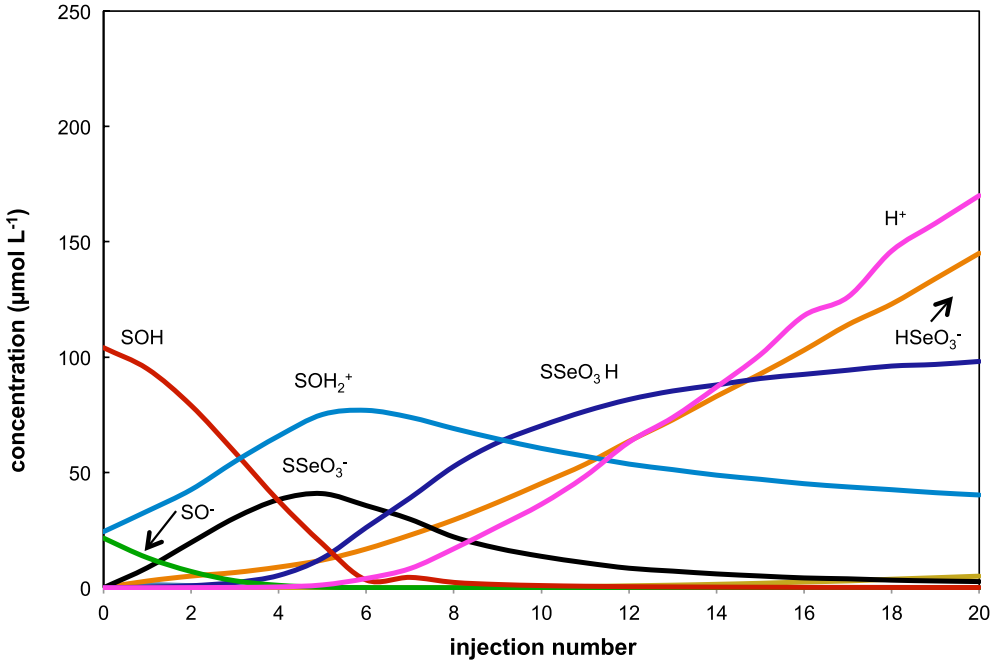

Figure 2. Aqueous and surface speciation curves for alumina and selenite system.

progressively to zero. The mass balance equations show that in both cases, $\equiv SSeO_3H$ is mainly formed from $\equiv SOH_2^+$ but as regards Al_2O_3 a small part also comes from the transformation of the $\equiv SSeO_3^-$ sites.

3.2. Enthalpies of sorption

3.2.1. Protonation of SeO_3^{2-} in solution

The calculations that will be carried out below in order to get the enthalpy of sorption do require the knowledge of the enthalpies of reactions (1) and (2). The enthalpies of formation of the species involved in these two reactions being known (Shock, Sassani, Willis, & Sverjensky, 1997), ΔH_1 and ΔH_2 can

be calculated. As a check, we have microcalorimetrically determined these values in 0.100 mol L^{-1} $NaNO_3$ aqueous solution by titrating an aliquot containing 0.020 mol L^{-1} Na_2SeO_3 with 0.051 mol L^{-1} HNO_3.

The power–time curve shown in Figure 3 evidences the exothermic enthalpy of first protonation ($\Delta H_1 < 0$) and the endothermic enthalpy of second protonation ($\Delta H_2 > 0$). By treating the microcalorimetric data with the DIGITAM 4.1 minimization software (Thermometric – TA Instruments), we obtain the enthalpies of first and second protonation with a satisfactory precision ($\Delta H_1 = -5.0 \pm 0.2$ kJ mol^{-1} and $\Delta H_2 = 6.2 \pm 0.5$ kJ mol^{-1}). These values are in good agreement with those calculated (−5.4 and 7.1 kJ mol^{-1}) from Shock's standard state data (Shock et al., 1997).

3.2.2. Formation of $SSeO_3H$ on alumina and montmorillonite

Figure 4 shows the power–time curve obtained upon addition of SeO_3^{2-} on MNa; a similar curve (not shown) was obtained upon addition on Al_2O_3, except that the peaks were smaller. In both cases, the heat effect is exothermic, small and almost constant upon each addition. As explained in Section 3.1, the enthalpy of sorption can only be extracted from the acidic range of the titration, that is between the 10th and 20th injections: by treating the microcalorimetric data with the DIGITAM 4.1 software, we can get the total heat corresponding to the summation of the integrals of the 10 last peaks of the power–time curve. Here are the average values obtained from several independent measurements: Q(MNa) = 15 mJ and Q(Al_2O_3) = 7 mJ. In both cases, the enthalpy change ($\Delta H = -Q$) corresponds to the process described by reaction (6) and the simultaneously occurring reactions (1) and (2). It can be expressed as a function of the extent of these reactions as follows

$$\Delta H = -Q = \left[\Delta n\left(SSeO_3H\right)\right] * \Delta H_6 + \left[\Delta n\left(HSeO_3^-\right)\right] * \Delta H_1 + \left[\Delta n\left(H_2SeO_3\right)\right] * \Delta H_2 \quad (7)$$

where Δn is the change of the number of moles of the considered species. The Δn values are calculated from the concentrations used to get the speciation curves (Figures 1 and 2) between the 10th and the 20th injections. The enthalpies of first and second protonation of SeO_3^{2-} in aqueous solution being known, it is then possible to extract ΔH_6 from Equation 7, both for alumina and montmorillonite.

Let us now try to estimate the uncertainty to which these results are subject. To do so, we start by assuming that the concentrations of the different species, which were determined on the basis of the model chosen to describe the chemical equilibria, are exact. Next, we assume that the enthalpy for the sorption of SeO_3^{2-} on the solid surface, that is ΔH_6, does not vary while the occupancy rate of the surface sites changes from 0.02 to 0.2 for the montmorillonite and from 0.06 to 0.7 for the alumina. As regards the microcalorimetric data, it must be underlined that, in Equation 7, the term corresponding to the first protonation of SeO_3^{2-} (exothermic) is almost 50 times larger (in absolute value) than that corresponding to the second protonation (endothermic) and is almost 100 times larger than the whole Q value itself

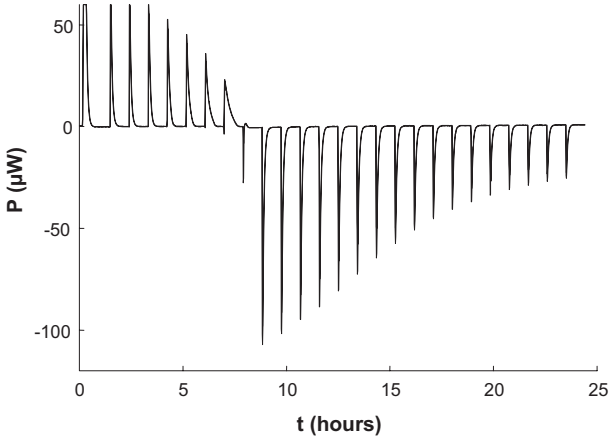

Figure 3. Power (heat flux)–time curve for the protonation of selenite in solution.

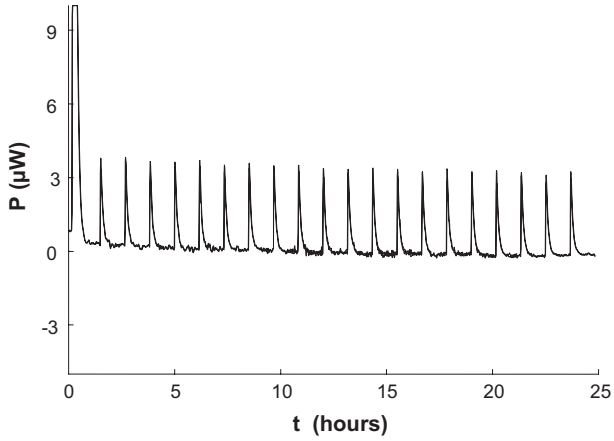

Figure 4. Power (heat flux)–time curve for the sorption of selenite on Na-montmorillonite.

(exothermic). This means that the exothermic first protonation of SeO_3^{2-} does essentially compensate the endothermic sorption. If we assume that the uncertainty on ΔH_1 is equal to ± 0.5 kJ mol^{-1}, which is consistent with the difference observed between our value and that given by Shock et al. (as reported in Section 3.2.1), this induces an error of ± 5 kJ mol^{-1} on the enthalpy of sorption. Considering the errors on the Δn and Q values and the dispersal of our results, we can propose the following ΔH_6 for the montmorillonite:

$$\Delta H_6(\text{MNa}) = 50 \pm 10\ \text{kJ mol}^{-1}$$

With Al_2O_3, there is an additional problem due to the fact that the sorbed species $SSeO_3^-$ does disappear according to the following equilibrium:

$$SSeO_3^- + H^+ = SSeO_3H \qquad (8)$$

However, this transformation regresses as the titration goes on and pH decreases. Therefore, the Δn values were calculated from the speciation data for the last injections (Figure 2: injection number varying from 15 to 20), which yielded the following ΔH_6 value for the alumina:

$$\Delta H_6\left(Al_2O_3\right) = 40 \pm 10\ \text{kJ mol}^{-1}$$

So, although the enthalpies of sorption of SeO_3^{2-} on the solid surface of montmorillonite and alumina in acidic medium (reaction (6)) are affected by important errors, it is obvious that both values are of the same order of magnitude and clearly endothermic.

3.2.3. Formation of $SSeO_3H$ and $SSeO_3^-$ on alumina

Let us now examine the sorption of SeO_3^{2-} on an alumina suspension whose concentration is increased 10-fold, that is 4 g L^{-1}. Under such conditions, the concentrations of the species at equilibrium and the sorption rates are larger than those previously surveyed. This is interesting because it allows us to check the effect of these parameters on ΔH_6 and also to scrutinize the $SSeO_3^-$ species and to assess ΔH_5. To simplify, we will not present here an analysis of the data as detailed as above but we will simply underline the major points observed upon two different microcalorimetric titrations of this more concentrated alumina suspension. For both titrations, the suspension was prepared, as before, in 0.100 mol L^{-1} $NaNO_3$ aqueous solution. 3 mL of this 4 g L^{-1} suspension was titrated by injection of a titrant prepared in the same solution and containing now 0.040 mol L^{-1} Na_2SeO_3 and 0.080 mol L^{-1} HNO_3.

The first titration was carried out by injecting 20 × 10 µL of titrant. Speciation curves analogous to those shown in Figure 2 were obtained, except for the concentration of $SSeO_3H$ which was higher on

the whole range and the concentration of $\equiv SSeO_3^-$ which was totally negligible between the 12th and 20th injections. This yielded the following value for the enthalpy of reaction (6):

$$\Delta H_6(Al_2O_3) = 40 \pm 5\ kJ\ mol^{-1}$$

It can be noticed that the value is the same as that found when the suspension was at a concentration of 0.40 g L^{-1} but, because the conditions are now more favourable, the uncertainty is twice smaller.

In order to define with more precision the initial part of this titration (between the first and fourth injections), during which the pH varies from 8.5 to 6.5 and where the two sorbed species ($\equiv SSeO_3H$ and $\equiv SSeO_3^-$) coexist, a second titration was carried out by injecting 10 × 4 µL of titrant. Using the enthalpy of reaction (6) given above, the enthalpies of the first and second protonation of the alumina surface determined previously (Morel et al., 2009), and the changes of the number of moles of the considered species, it was then possible to calculate the enthalpy of reaction (5) from :

$$\Delta H = -Q = \left[\Delta n(\equiv SSeO_3H)\right] * \Delta H_6 + \left[\Delta n(\equiv SSeO_3^-)\right] * \Delta H_5 + \left[\Delta n(HSeO_3^-)\right] * \Delta H_1 + \left[\Delta n(H_2SeO_3)\right] * \Delta H_2 \quad (9)$$

This yielded:

$$\Delta H_5(Al_2O_3) = 35 \pm 5\ kJ\ mol^{-1}$$

So by working on a more concentrated suspension, we have been able to confirm the enthalpy of reaction (6) but also to determine the enthalpy of reaction (5). It can be noticed that the enthalpies of sorption of the selenite ion on alumina in neutral (ΔH_5) and in acidic (ΔH_6) media are nearly the same.

3.3. Sorption curves

3.3.1 Experimental curves

In order to facilitate the comparison between alumina and MNa, the sorption of Se(IV) is expressed with the distribution coefficient K_d given by:

$$K_d = \frac{Se(IV)_{sorbed-per-gram-of-solid}}{Se(IV)_{dissolved-per-litre-of-solution}} \quad (10)$$

Figures 5 and 6 show K_d as a function of pH for alumina and MNa at 25 and 40°C, respectively. The shape of the curves corresponds to the classical behaviour of an oxoanion which is more strongly sorbed on a mineral surface at low pH. For the same ratio $Se(IV)_{initial-concentration}$/*number of surface sites*, the sorption on alumina is stronger than on MNa, which is due to the higher electrostatic contribution caused by the alumina surface sites surrounding.

3.3.2. Calculated curves

The thermodynamic data from Table 2 can account for the sorption behaviour of Se(IV) on alumina and MNa at 25°C (Figure 5). By introducing into the van't Hoff relation the enthalpies of sorption determined by microcalorimetry and the *K* values measured at 25°C, it is possible to deduce the equilibrium constants for the sorption of Se at 40°C (Table 2).

As was done previously for europium (Morel et al., 2012), the curve at 40°C was predicted by introducing in the FITEQL 4.0 code the surface sites density and specific area listed in Table 1 for alumina and montmorillonite and the values of K_1, K_2, K_3, K_4, K_5 and K_6 calculated at 40°C from the van't Hoff relation. The sorption curves thus obtained at 40°C are compared to the experimental sorption data in Figure 6 where they show, in particular, that they do account for the higher electrostatic contribution caused by the alumina surface sites surrounding with a good precision. It must be underlined that the sorption curves shown in these figures have been calculated without any fitted parameter

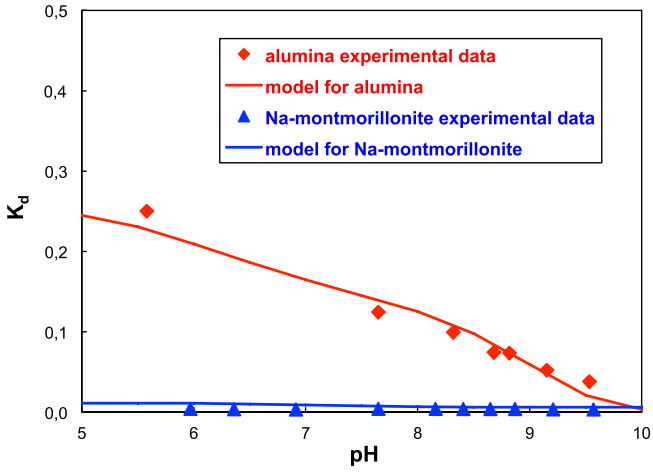

Figure 5. Sorption of Se(IV) on alumina and Na-montmorillonite as a function of pH at 25°C.

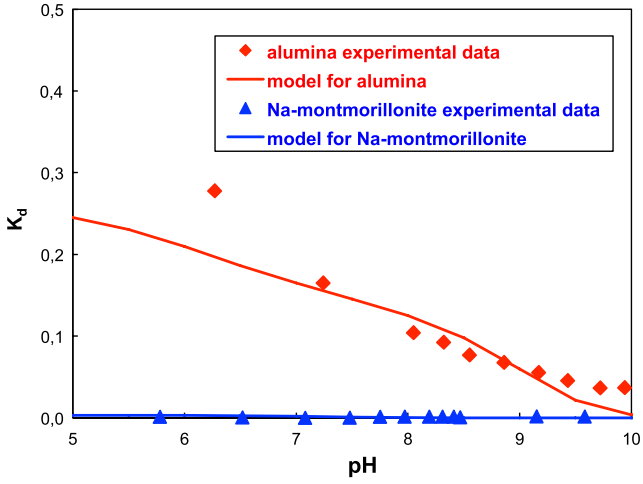

Figure 6. Sorption of Se(IV) on alumina and Na-montmorillonite as a function of pH at 40°C.

and that, even if approximations and simplifications are numerous in this predictive calculation, these calculated curves are in good agreement with the experimental ones.

3.4. Thermodynamic parameters for the sorption of SeO_3^{2-} *on aluminol sites*

The surface complexation of SeO_3^{2-} is represented by a combination of both reactions (5) and (6). The experimental findings have shown that reaction (5) prevails in neutral or slightly acidic medium but that the situation is reversed in more acidic medium, reaction (6) becoming more and more predominant as the pH decreases. The standard thermodynamic parameters that characterize these sorption reactions at 25°C have been deduced from the data reported in Table 2 and have been collected in Table 3.

Table 3. Standard thermodynamic parameters for the sorption of SeO_3^{2-} on aluminol sites at 25°C*

Reaction	ΔG° (kJ mol⁻¹)	ΔH° (kJ mol⁻¹)	TΔS° (kJ mol⁻¹)
$SOH_2^+ + SeO_3^{2-} = SSeO_3^- + H_2O$	25	35	10
$SOH_2^+ + SeO_3^{2-} + H^+ = SSeO_3H + H_2O$	64	40	−24

*The aluminol sites, designed by SOH, were considered identical for alumina and Na-montmorillonite (see text).

The standard free energy is markedly more unfavourable for reaction (6) than for reaction (5). The enthalpies of both reactions being of the same order of magnitude, it is the negative entropy of reaction (6) that explains the difference.

4. Conclusion

The present study aimed to find a simple way to predict the temperature effect on the thermodynamics of selenium sorption on alumina and montmorillonite. In order to do so, batch experiments were carried out to get the equilibrium constants at 25 and 40°C and microcalorimetry was used to determine the enthalpy changes upon sorption. Two hypotheses were made to treat the experimental data : a simple surface complexation model was used, which assumes that the thermodynamic properties of the aluminol surface sites of both alumina and montmorillonite are identical, and it was supposed that the van't Hoff relation can reliably be applied both to the homogeneous and heterogeneous reactions that occur during the sorption process. The experimental data showed that the surface complexation of SeO_3^{2-}, which is represented by a combination of both reactions (5) and (6), is modulated by pH: reaction (5) does prevail in neutral or slightly acidic medium but the situation is reversed in more acidic medium, reaction (6) becoming more and more predominant as the pH decreases. The enthalpies of sorption in neutral (ΔH_5) and in acidic (ΔH_6) media were deduced from the microcalorimetric data and appeared to be endothermic and nearly the same. By introducing the enthalpies of sorption and the K values measured at 25°C into the van't Hoff relation, it was possible to calculate the equilibrium constants at 40°C and these calculated values showed to be in good agreement with the experimental ones. This demonstrates the validity of the above assumptions for the prediction of the temperature effect on the sorption of selenium on alumina and montmorillonite.

Funding
This work was funded by the French Ministry of Higher Education and Research (MESR) and by the National Center for Scientific Research (CNRS).

Author details
Jean-Pierre Morel[1]
E-mail: J-Pierre.MOREL@univ-bpclermont.fr
Nicolas Marmier[2]
E-mail: Nicolas.MARMIER@unice.fr
Charlotte Hurel[2]
E-mail: Charlotte.HUREL@unice.fr
Nicole Morel-Desrosiers[1]
E-mail: Nicole.MOREL@univ-bpclermont.fr
[1] Université Clermont Auvergne - Université Blaise Pascal, Laboratoire Microorganismes: Génome et Environnement, UMR CNRS 6023, BP 10448, 63000 Clermont-Ferrand, France.
[2] Université Nice Sophia Antipolis, ECOMERS, EA 4228, 28 avenue de Valrose, 06108 Nice cedex 2, France.

Citation information
Cite this article as: Thermodynamics of selenium sorption on alumina and montmorillonite, Jean-Pierre Morel, Nicolas Marmier, Charlotte Hurel & Nicole Morel-Desrosiers, *Cogent Chemistry* (2015), 1: 1070943.

References

Alessi, D. S., & Fein, J. B. (2009). Cadmium adsorption to mixtures of soil components: Testing the component additivity approach. *Chemical Geology, 270*, 186–195.
Bingham, P. A., Connelly, A. J., Cassingham, N. J., & Hyatt, N. C. (2010). Oxidation state and local environment of selenium in alkali borosilicate glasses for radioactive waste immobilisation. *Journal of Non-Crystalline Solids, 357*, 2726–2734.
Cornelis, G., Poppe, S., Van Gerven, T., Van den Broeck, E., Ceulemans, M., & Vandecasteele, C. (2008). Geochemical modelling of arsenic and selenium leaching in alkaline water treatment sludge from the production of non-ferrous metals. *Journal of Hazardous Materials, 159*, 271–279. http://dx.doi.org/10.1016/j.jhazmat.2008.02.016
Davis, J. A., Meece, D. E., Kohler, M., & Curtis, G. P. (2004). Approaches to surface complexation modeling of Uranium(VI) adsorption on aquifer sediments. *Geochimica et Cosmochimica Acta, 68*, 3621–3641. http://dx.doi.org/10.1016/j.gca.2004.03.003
de Llano, A. Y., Bidoglio, G., Avogadro, A., Gibson, P. N., & Rivas Romero, P. (1996). Redox reactions and transport of selenium through fractured granite. *Journal of Contaminant Hydrology, 21*, 129–139. http://dx.doi.org/10.1016/0169-7722(95)00038-0
Fujimoto, Y., Morinaga, K., Abe, M., Kitamura, T., & Sakuma, S. (2009). Selenite induces oxidative DNA damage in primary rat hepatocyte cultures. *Toxicology Letters, 191*, 341–346. http://dx.doi.org/10.1016/j.toxlet.2009.10.001
Goldberg, S., Lesch, S. M., & Suarez, D. L. (2007). Predicting selenite adsorption by soils using soil chemical parameters in the constant capacitance model. *Geochimica et Cosmochimica Acta, 71*, 5750–5762. http://dx.doi.org/10.1016/j.gca.2007.04.036
Herbelin, A. L., & Westall, J. C. (1999). A computer program for determination of chemical equilibrium constants from experimental data (Version 4.0). Corvallis, OR: Department of Chemistry, Oregon State University.
Hurel, C., Marmier, N., Séby, F., Giffaut, E., Bourg, A. C. M., & Fromage, F. (2002). Sorption behaviour of caesium on a bentonite sample. *Radiochimica Acta, 90*, 695–698.
Johnston, P. A. (1987). Acute toxicity of inorganic selenium to Daphnia magna (Straus) and the effect of sub-acute exposure upon growth and reproduction. *Aquatic Toxicology, 10*, 335–352. http://dx.doi.org/10.1016/0166-445X(87)90007-5
Jordan, N., Marmier, N., Lomenech, C., Giffaut, E., & Ehrhardt, J.-J. (2009). Competition between selenium (IV) and silicic acid on the hematite surface. *Chemosphere, 75*, 129–134. http://dx.doi.org/10.1016/j.chemosphere.2008.11.018
Kumar, A. R., & Riyazuddin, P. (2011). Speciation of selenium in groundwater: Seasonal variations and redox transformations. *Journal of Hazardous Materials, 192*, 263–269.

Landry, C. J., Koretsky, C. M., Lund, T. J., Schaller, M., & Das, S. (2009). Surface complexation modeling of Co(II) adsorption on mixtures of hydrous ferric oxide, quartz and kaolinite. *Geochimica et Cosmochimica Acta, 73*, 3723–3737. http://dx.doi.org/10.1016/j.gca.2009.03.028

Lyklema, J. J., de Keizer, A., Bijsterbosch, B. H., Fleer, G. J., & Cohen Stuart, M. A. (1995). *Fundamentals of interface and colloid science, Volume 2: Solid–liquid interfaces* (Part 3 Electric double layers, pp. 1–232). San Diego, CA: Academic Press.

Ma, Y., Wu, M., Li, D., Li, X.-q., Li, P., Zhao, J., … Ma, X. (2012). Embryonic developmental toxicity of selenite in zebrafish (*Danio rerio*) and prevention with folic acid. *Food and Chemical Toxicology, 50*, 2854–2863. http://dx.doi.org/10.1016/j.fct.2012.04.037

Marmier, N., Dumonceau, J., Chupeau, J., & Fromage, F. (1994). Effect of electrostatic constraints on the sorption of trivalent ytterbium on alumina. *Comptes Rendus de l'Academie des Sciences, Serie IIb: Mecanique, Physique, Chimie, Astronomie, 318*, 177–183.

Morel, J.-P., Marmier, N., Hurel, C., & Morel-Desrosiers, N. (2006). Effect of temperature on the acid-base properties of the alumina surface: Microcalorimetry and acid-base titration experiments. *Journal of Colloid and Interface Science, 298*, 773–779. http://dx.doi.org/10.1016/j.jcis.2006.01.022

Morel, J.-P., Marmier, N., Hurel, C., & Morel-Desrosiers, N. (2009). Acid-base properties of the alumina surface: Influence of the titration procedures on the microcalorimetric results. *Journal of Colloid and Interface Science, 338*, 10–15. http://dx.doi.org/10.1016/j.jcis.2009.06.059

Morel, J.-P., Marmier, N., Hurel, C., & Morel-Desrosiers, N. (2012). Effect of temperature on the sorption of europium on alumina: Microcalorimetry and batch experiments. *Journal of Colloid and Interface Science, 376*, 196–201. http://dx.doi.org/10.1016/j.jcis.2012.02.035

Morlon, H., Fortin, C., Floriani, M., Adam, C., Garnier-Laplace, J., & Boudou, A. (2005). Toxicity of selenite in the unicellular green alga Chlamydomonas reinhardtii: Comparison between effects at the population and sub-cellular level. *Aquatic Toxicology, 73*, 65–78. http://dx.doi.org/10.1016/j.aquatox.2005.02.007

Peak, D. (2006). Adsorption mechanisms of selenium oxyanions at the aluminum oxide/water interface. *Journal of Colloid and Interface Science, 303*, 337–345. http://dx.doi.org/10.1016/j.jcis.2006.08.014

Ryu, J.-H., Gao, S., & Tanji, K. K. (2011). Accumulation and speciation of selenium in evaporation basins in California, USA. *Journal of Geochemical Exploration, 110*, 216–224. http://dx.doi.org/10.1016/j.gexplo.2011.05.011

Schaller, M. S., Koretsky, C. M., Lund, T. J., & Landry, C. J. (2009). Surface complexation modeling of Cd(II) adsorption on mixtures of hydrous ferric oxide, quartz and kaolinite. *Journal of Colloid and Interface Science, 339*, 302–309. http://dx.doi.org/10.1016/j.jcis.2009.07.053

Séby, F., Potin-Gautier, M., Giffaut, E., Borge, G., & Donard, O. F. X. (2001). A critical review of thermodynamic data for selenium species at 25°C. *Chemical Geology, 171*, 173–194. http://dx.doi.org/10.1016/S0009-2541(00)00246-1

Séby, F., Potin Gautier, M., Lespés, G., & Astruc, M. (1997). Selenium speciation in soils after alkaline extraction. *Science of The Total Environment, 207*, 81–90. http://dx.doi.org/10.1016/S0048-9697(97)00269-6

Shock, E. L., Sassani, D. C., Willis, M., & Sverjensky, D. A. (1997). Inorganic species in geologic fluids: Correlations among standard molal thermodynamic properties of aqueous ions and hydroxide complexes. *Geochimica et Cosmochimica Acta, 61*, 907–950. http://dx.doi.org/10.1016/S0016-7037(96)00339-0

Tinggi, U. (2003). Essentiality and toxicity of selenium and its status in Australia: A review. *Toxicology Letters, 137*, 103–110. http://dx.doi.org/10.1016/S0378-4274(02)00384-3

Torres, J., Pintos, V., Gonzatto, L., Dominguez, S., Kremer, C., & Kremer, E. (2011). Selenium chemical speciation in natural waters: Protonation and complexation behavior of selenite and selenate in the presence of environmentally relevant cations. *Chemical Geology, 288*, 32–38.

Um, W., Serne, R. J., Brown, C. F., & Rod, K. A. (2008). Uranium(VI) sorption on iron oxides in Hanford Site sediment: Application of a surface complexation model. *Applied Geochemistry, 23*, 2649–2657. http://dx.doi.org/10.1016/j.apgeochem.2008.05.013

Wen, H., & Carignan, J. (2007). Reviews on atmospheric selenium: Emissions, speciation and fate. *Atmospheric Environment, 41*, 7151–7165. http://dx.doi.org/10.1016/j.atmosenv.2007.07.035